NeuroImage xxx (2014) xxx–xxx

Contents lists available at ScienceDirect

NeuroImage

journal homepage: www.elsevier.com/locate/ynimg

Comparison of structural covariance with functional connectivity approaches exemplified by an investigation of the left anterior insula

Mareike Clos [a,b], Claudia Rottschy [a,c], Angela R. Laird [d], Peter T. Fox [e,f], Simon B. Eickhoff [a,g,*]

[a] Institute of Neuroscience and Medicine (INM-1), Research Centre Jülich, Jülich, Germany
[b] Department of Systems Neuroscience, University Medical Center Hamburg-Eppendorf, Hamburg, Germany
[c] Department of Psychiatry, Psychotherapy and Psychosomatics, RWTH Aachen University Hospital, Aachen, Germany
[d] Department of Physics, Florida International University, Miami, FL, USA
[e] Research Imaging Institute, University of Texas Health Science Center at San Antonio, TX, USA
[f] South Texas Veterans Administration Medical Center, San Antonio, TX, USA
[g] Institute of Clinical Neuroscience and Medical Psychology, Heinrich Heine University, Düsseldorf, Germany

ARTICLE INFO

Article history:
Accepted 9 May 2014
Available online xxxx

Keywords:
BrainMap
fMRI
Meta-analytic connectivity modeling (MACM)
Resting state
Schizophrenia

ABSTRACT

The anterior insula is a multifunctional region involved in various cognitive, perceptual and socio-emotional processes. In particular, a portion of the left anterior insula is closely associated with working memory processes in healthy participants and shows gray matter reduction in schizophrenia. To unravel the functional networks related to this left anterior insula region, we here combined resting state connectivity, meta-analytic-connectivity modeling (MACM) and structural covariance (SC) in addition to functional characterization based on BrainMap meta-data. Apart from allowing new insight into the seed region, this approach moreover provided an opportunity to systematically compare these different connectivity approaches. The results showed that the left anterior insula has a broad response profile and is part of multiple functional networks including language, memory and socio-emotional networks. As all these domains are linked with several symptoms of schizophrenia, dysfunction of the left anterior insula might be a crucial component contributing to this disorder. Moreover, although converging connectivity across all three connectivity approaches for the left anterior insula were found, also striking differences were observed. RS and MACM as functional connectivity approaches specifically revealed functional networks linked with internal cognition and active perceptual/language processes, respectively. SC, in turn, showed a clear preference for highlighting regions involved in social cognition. These differential connectivity results thus indicate that the use of multiple forms of connectivity is advantageous when investigating functional networks as conceptual differences between these approaches might lead to systematic variation in the revealed functional networks.

Introduction

The anterior insula (AI) is a multifunctional integration region that has been associated with various sensory, cognitive and socio-affective processes (Kurth et al., 2010; Mutschler et al., 2009) and is hypothesized to implement the integration of external and internal processes by large-scale interactions with other brain regions (Craig, 2009; Menon and Uddin, 2010; Singer et al., 2009). Moreover, two recent meta-analyses highlighted the left AI as a core region in working memory (Rottschy et al., 2012) and as a region displaying structural abnormalities in schizophrenia (Nickl-Jockschat et al., 2011). This left AI region thus seems to be a key component of cognitive functioning in healthy subjects and shows aberrations in a highly prevalent mental disorder, prompting questions about the functional networks associated with it.

When aiming to delineate the functional interactions of this region, it is noteworthy that functional connectivity analysis is actually a rather heterogeneous construct. In particular, there are several different approaches to detect functional networks on the basis of non-invasive neuroimaging. Firstly, task-free resting state (RS) connectivity can be used to reveal brain regions that display temporal correlations with the seed region in functional MRI time-series obtained while no explicit task is presented (Fox and Raichle, 2007; Smith et al., 2013). Secondly, task-based functional connectivity using meta-analytic co-activation modelling (MACM) has been established as another functional connectivity approach (Eickhoff et al., 2010; Laird et al., 2013). Here, co-activation of regions with a certain seed region across many experiments recorded in the BrainMap database (Fox and Lancaster, 2002; Laird et al., 2005, 2009, 2011) is used to identify functional networks. Furthermore, the meta-data specifying the kind of task and contrast

* Corresponding author at: Forschungzentrum Jülich, INM-1, 52425 Jülich, Germany. Fax: +49 2461 61–2990.
E-mail address: s.eickhoff@fz-juelich.de (S.B. Eickhoff).

http://dx.doi.org/10.1016/j.neuroimage.2014.05.030
1053-8119/

employed by experiments activating the region of interest may be used to functionally characterize the resulting networks and thus reveal their functional implication. Thirdly, structural covariance (SC) is an analysis method to infer structural networks which in turn result from to a combination of genetic, maturational and functional interaction effects (Evans, 2013). As such, the examination of SC networks can possibly contribute to the understanding of functional connectivity, although it is not yet entirely clear to what degree structural covariance can directly infer functional networks. In particular, this approach is based on the correlation of gray matter characteristics such as volume or thickness across participants (Albaugh et al., 2013; Lerch et al., 2006). Conceptually, gray matter covariance is thought to reflect shared maturational and functional specialization processes of these regions in addition to genetic factors (Alexander-Bloch et al., 2013; Evans, 2013). Such structural covariance patterns have been shown to exist between brain regions belonging to the same functional system in healthy participants (Andrews et al., 1997; Mechelli et al., 2005). Moreover, the learning of specific skills has been demonstrated to lead to training-induced structural plasticity in the networks subserving these skills (Draganski et al., 2004; Driemeyer et al., 2008; Haier et al., 2009; Maguire et al., 2003). Also in patient populations specific structural covariance abnormalities have been observed (Bernhardt et al., 2008; Bullmore et al., 1998; Mitelman et al., 2005; Spreng and Turner, 2013). In this context, it needs to be stressed that all three approaches – RS, MACM and SC – share the same goal of delineating regions that interact with the seed. In spite of this shared goal, however, substantial conceptual differences are also evident and in particular for SC there is still some debate regarding the extent that anatomical covariance networks represent functional connectivity. While there has been some evidence for convergence between RS and MACM (Cauda et al., 2011; Hoffstaedter et al., 2014; Jakobs et al., 2012), between RS and SC (He et al., 2007; Seeley et al., 2009), as well as between RS, MACM and SC onto a common insular architecture (Kelly et al., 2012), a systematic comparison of all these three approaches is still lacking. Such a comparison, however, seems highly warranted given the increasing focus on network interactions in neuroimaging (Kousta, 2013) and the conceptual differences between the approaches. In particular, these raise the question to which degree these methods may reveal common but also differential interactions, i.e., whether there is a bias in the delineated networks. A multimodal region such as the left AI might be particularly suited to tackle this question as it offers the possibility to discern multiple functional networks that could be preferentially delineated by the different conceptual approaches to functional connectivity. We thus examined RS-, MACM- and SC-derived networks seeded from the left AI as defined by two previous meta-analyses on working memory activations (Rottschy et al., 2012) and atrophy in schizophrenia (Nickl-Jockschat et al., 2011).

Material and methods

VOI definition and functional characterization

The seed volume of interest (VOI) was based on converging findings in the left anterior insula reported in two meta-analyses. The first identified the anterior insula as one of four regions showing significant reductions in gray matter volume in patients with schizophrenia compared with healthy controls across 38 morphometric MRI studies (Nickl-Jockschat et al., 2011). Secondly, the anterior insula was one of the core regions for working memory as identified in a meta-analysis across 189 task-based fMRI studies (Rottschy et al., 2012). We computed the intersection between the left anterior insula (AI) volumes resulting from these two meta-analyses and used this overlap as a seed VOI for the current study (Fig. 1A). The seed region was thus not explicitly drawn around the centre MNI coordinates but determined by this intersection between the two volumes. This intersection volume had an extent of 90 voxels at 2 x 2 x 2 mm resolution. As this overlap between the two volumes was fully localized in the left anterior insula, no additional steps were necessary to ensure that the AI seed region was limited to the insula.

We furthermore functionally characterized the AI seed region based on the Behavioral Domain and Paradigm Class meta-data from the BrainMap database (http://www.brainmap.org; Fox and Lancaster, 2002; Laird et al., 2009, 2011). Behavioral domains include the main categories cognition, action, perception, emotion, and interoception, as well as their related sub-categories. Paradigm classes categorize the specific task employed (see http://brainmap.org/scribe for more information on the BrainMap taxonomy). The functional profile was determined using forward and reverse inference. Forward inference is the probability of observing activity in a brain region given knowledge of the psychological process, whereas reverse inference is the probability of a psychological process being present given knowledge of activation in a particular brain region. In the forward inference approach, the functional profile was determined by identifying taxonomic labels for which the probability of finding activation in the respective region was significantly higher than the overall (a priori) chance across the entire database. That is, we tested whether the conditional probability of activation given a particular label [P(Activation|Task)] was higher than the baseline probability of activating the region in question per se [P(Activation)]. Significance was established using a binomial test ($p < 0.05$, corrected for multiple comparisons using FDR; Müller et al., 2013; Rottschy et al., 2013). In the reverse inference approach, the functional profile was determined by identifying the most likely behavioral domains and paradigm classes given activation in a particular region. This likelihood P(Task|Activation) can be derived from P(Activation|Task) as well as P(Task) and P(Activation) using Bayes rule. Significance (at $p < 0.05$, corrected for multiple comparisons using FDR; Müller et al., 2013; Rottschy et al., 2013) was then assessed by means of a chi-squared test.

Resting state functional connectivity

Task-independent functional connectivity of the anterior insula was investigated by means of a seed based resting state (RS) analysis. RS fMRI images of 132 healthy volunteers between 18 and 85 years (mean age 42.3 ± 18.08 years; 78 males) from the NKI/Rockland sample were obtained through the 1000 Functional Connectomes project (www.nitrc.org/projects/fcon_1000/; Nooner et al., 2012). During the RS scans subjects were instructed to keep their eyes closed and to think about nothing in particular but not to fall asleep. For each subject 260 RS EPI images were acquired on a Siemens TimTrio 3 T scanner using blood-oxygen-level-dependent (BOLD) contrast [gradient-echo EPI pulse sequence, TR = 2.5 s, TE = 30 ms, flip angle = 80°, in plane resolution = 3.0 x 3.0 mm^2, 38 axial slices (3.0 mm thickness) covering the entire brain]. The first four scans were excluded from further processing analysis using SPM8 to allow for magnet saturation. The remaining EPI images were first corrected for movement artifacts by affine registration using a two pass procedure in which the images were first aligned to the initial volumes and subsequently to the mean after the first pass. No slice time correction was applied as this correction has minimal effect on functional connectivity (Wu et al., 2011). The mean EPI of each subject was then spatially normalized to the MNI single subject template using the "unified segmentation" (Ashburner and Friston, 2005). The ensuing deformation was applied to the individual EPI volumes. To improve signal-to-noise ratio and to compensate for residual anatomical variations the images were smoothed with a 5-mm FWHM Gaussian kernel.

The time-series data of each voxel were processed as follows (Satterthwaite et al., 2013): In order to reduce spurious correlations, variance that could be explained by the following nuisance variables was removed: i) the six motion parameters derived from the image realignment; ii) the first derivative of the realignment parameters; and iii) mean gray matter, white matter and CSF signal per time-point as

Please cite this article as: Clos, M., et al., Comparison of structural covariance with functional connectivity approaches exemplified by an investigation of the left anterior i..., NeuroImage (2014), http://dx.doi.org/10.1016/j.neuroimage.2014.05.030

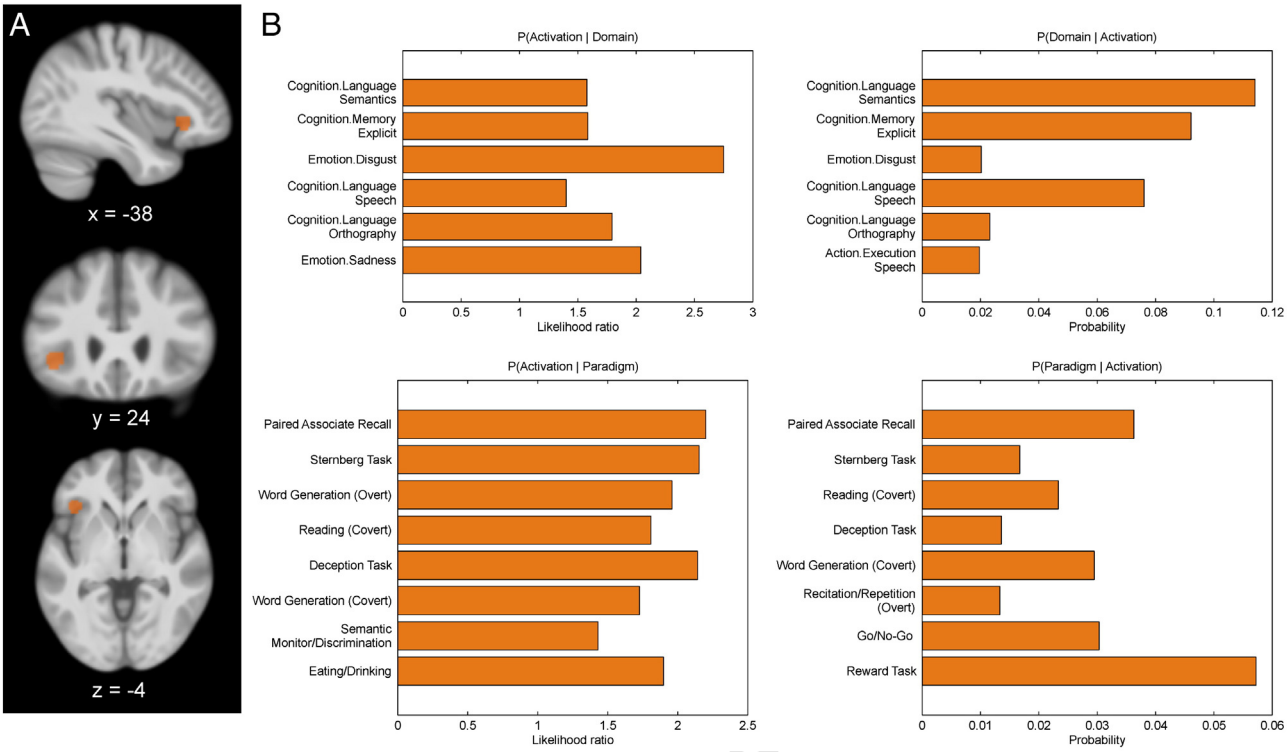

Fig. 1. The left anterior insula seed. (A) The left anterior insula seed displayed on sagittal, coronal and axial sections of the mean anatomical image of the NKI sample. *x*, *y* and *z* values represent the center of gravity in MNI space. (B) Behavioral domains (upper row) and paradigm classes (lower row) from the BrainMap database significantly associated with the anterior insula seed (uncorrected $p < 0.05$).

obtained by averaging across voxels attributed to the respective tissue class in the SPM8 segmentation (Clos et al., 2014). All nuisance variables entered the model as first and second order terms. Data was then band pass filtered preserving frequencies between 0.01 and 0.08 Hz, since meaningful resting state correlations will predominantly be found in these frequencies given that the BOLD response acts as a low-pass filter (Biswal et al., 1995; Fox and Raichle, 2007).

The time-course was extracted from the left AI seed volume for every subject by computing the first eigenvariate of the time-series of those 50% of the seed's gray matter voxels (median split) that had the highest probabilities of representing gray matter according to the SPM8 segmentation. To quantify RS functional connectivity, linear (Pearson) correlation coefficients were computed between this seed time-series and the time-series of all other gray matter voxels in the brain (Reetz et al., 2012; zu Eulenburg et al., 2012). The voxel-wise correlation coefficients were then transformed into Fisher's Z-scores and tested for consistency across subjects by a second-level analysis of variance (ANOVA, including appropriate non-sphericity correction). The results of this random-effects analysis were family-wise error (FWE) corrected at a cluster level threshold of $p < 0.05$ (cluster-forming threshold: $p < 0.001$ at voxel level).

Meta-analytic connectivity modeling

Meta-analytic connectivity modeling (MACM) is a relatively new approach to the analysis of functional connectivity that assesses the correlations of neural activity in different brain areas over studies, i.e., co-activation (Eickhoff et al., 2010). MACM draws upon the advantage of high standardization in the publication of neuroimaging data, e.g., the ubiquitous adherence to standard coordinate systems (Talairach, MNI) and the emergence of large-scale databases that store this information. The key idea behind MACM is to first identify all experiments in a database that activate a particular brain region (seed VOI), and then test for convergence across (all) activation foci reported in these experiments (Eickhoff et al., 2010). Obviously, as experiments were selected by activation in the seed, highest convergence will be observed in the seed region. Significant convergence of the reported foci in other brain regions, however, indicates consistent co-activation over experiments with the AI seed region. To identify studies reporting neural activation within the AI region we used the BrainMap database (http://www.brainmap.org; Fox and Lancaster, 2002; Laird et al., 2009, 2011). To date, this database contained activation coordinates from over 10,000 neuroimaging experiments. Of these only imaging studies which examined task-based activations in a group of healthy subjects were considered, while between-group contrasts, patient populations and intervention-studies were excluded. These criteria yielded ~7200 eligible experiments at the time of analysis. As the first step of the MACM analysis we identified all experiments that featured at least one focus of activation within the AI VOI. The convergence of reported neural activation across the retrieved experiments was then modeled using the revised version of the activation likelihood estimation (ALE) algorithm (Eickhoff et al., 2009b).

The ALE approach is based on modeling the coordinates reported in the identified experiments as centers of 3D Gaussian probability distributions. These modeled activation fields reflect spatial uncertainties due to between-subject variability but also additional uncertainty caused by differences in spatial normalization and data analysis across single experiments (between-template variance). For each experiment, the probability distributions of all reported foci are combined into a modeled activation (MA) map (Turkeltaub et al., 2012). Taking the union across these MA maps yields voxel-wise ALE scores representing a quantitative description of activity convergence over all experiments at each particular location of the brain. To distinguish "true" convergence from random convergence, ALE scores are compared to an analytically derived null distribution reflecting a random spatial association between experiments [random effects analysis (Eickhoff et al., 2012)]. The ALE maps reflecting the convergence of co-activations with the AI VOI were family-wise error (FWE) corrected using the same statistical criteria as employed for the resting-state imaging data, i.e., at a cluster

Please cite this article as: Clos, M., et al., Comparison of structural covariance with functional connectivity approaches exemplified by an investigation of the left anterior i..., NeuroImage (2014), http://dx.doi.org/10.1016/j.neuroimage.2014.05.030

level threshold of $p < 0.05$ (cluster-forming threshold: $p < 0.001$ at voxel level), and converted to Z-scores for visualization.

Structural covariance

Structural covariance (SC) is based on the assumption that correlation between regional gray matter properties such as volume or cortical thickness across subjects is indicative of functional connectivity between these regions (Alexander-Bloch et al., 2013; Evans, 2013; He et al., 2007; Lerch et al., 2006). In particular, significant covariance of gray matter volume across individuals is thought to reflect shared developmental or recruitment and hence functional specialization of the respective regions (Alexander-Bloch et al., 2013; Zielinski et al., 2010). SC thus forms an alternative route to detect functional brain networks in vivo by reflecting the integrated effects of co-recruitment.

In order to investigate the brain-wide pattern of structural covariance with the AI seed, we used the anatomical T1-weighted images from the same subjects as described above for the RS analysis. For each of the 132 subjects T1-weighted images were acquired in sagittal orientation on a Siemens TimTrio 3 T scanner using an MP-RAGE sequence (TR = 2.5 s, TE = 3.5 ms, TI = 1200 ms, flip angle = 8°, FOV = 256 mm (256 x 256 matrix), 192 slices, voxel size 1 x 1 x 1 mm). The anatomical scans were preprocessed using the VBM8 toolbox (dbm.neuro.uni-jena.de/vbm) in SPM8 using standard settings (DARTEL normalization, spatially adaptive non-linear means denoising, a Markov random field weighting of 0.15 and bias field modeling with a regularization term of 0.0001 and a 60 mm FWHM cutoff). The resulting normalized gray matter segments, modulated only for the non-linear components of the deformations into standard space, were smoothed using an 8 mm isotropic FWHM kernel. This smoothing kernel differs admittedly from the 5 mm kernel used for the RS data; however, smaller kernels around 5 mm for functional data and larger kernels around 10 mm for structural data have been employed previously in combined RS and structural studies (Kelly et al., 2012; Seeley et al., 2009). Furthermore, identical kernels do not guarantee identical smoothness, as the intrinsic smoothness of the functional and structural data will be different. Subsequently, these normalized and smoothed gray matter segments were statistically analyzed by non-parametrical statistics using the "permute" function in FSL. In particular, we first computed the volume of the AI seed by integrating the modulated voxel-wise gray matter probabilities at the voxels corresponding to the seed cluster for each subject. This vector of subject-specific local volumes for the AI seed represented the covariate of interest in the statistical group analysis. The statistical analysis thus tested for each voxel whether the local volume at that particular voxel was significantly related to the volume of the AI. In the statistical model, we included age as a covariate of non-interest. In turn, as we modulated the gray matter probability maps by the non-linear components only to represent the absolute amount of tissue corrected for individual brain size, we did not include total brain volume as an additional covariate in the analysis. That is, given that the correction for inter-individual differences in brain volume was applied directly to the data it was not performed (a second time) as part of the statistical model. While we used cluster-level FWE correction at $p < 0.05$ for the RS and MACM data, this thresholding method is not valid for VBM data because cluster level correction requires stationary smoothness of the data, which cannot be assumed for VBM data (Ridgway et al., 2008). Therefore, we chose the currently recommended cluster-based correction for VBM data, namely threshold-free cluster enhancement (TFCE; Smith and Nichols, 2009). Significance was thus evaluated at $p < 0.05$ (corrected for multiple comparisons using full permutation testing of TFCE images) as implemented in FSL.

Comparison of connectivity measures

Common connectivity with the AI across the three evaluated modalities (RS, MACM, SC) was identified by computing the overlap between the thresholded connectivity maps using a minimum statistic conjunction (Nichols et al., 2005; conjunction null). Pair-wise differences at $p < 0.05$ were evaluated by computing contrasts between the connectivity maps and inclusively masking the resulting map with the thresholded connectivity map of interest. That is, regions that showed stronger RS than MACM connectivity were identified by computing the differences RS − MACM and masking by the main effect of RS. Finally, for each of the three connectivity approaches, we performed a conjunction analysis across the contrasts with the two other connectivity maps to highlight connected regions specific to RS, MACM and SC, respectively. For example, computing MACM − RS in conjunction with MACM − SC and the main effect of MACM identified regions specific to MACM. All resulting conjunction and contrast maps were additionally thresholded with a cluster extent threshold of 100 voxels. Finally, the resulting commonly and specifically connected regions were functionally characterized based on the Behavioral Domain and Paradigm Class meta-data from the BrainMap database as outlined above for the AI seed region.

Results

The functional characterization of the left AI revealed no significant associations with any specific behavioral domain or paradigm class at $p < 0.05$ (FDR-corrected for multiple comparisons) indicating a broad functional response profile. At $p < 0.05$ uncorrected, the BrainMap meta-data pointed to a role of this region in (working) memory, emotions and particularly in language and speech processes (Fig. 1B), confirming a relatively broad involvement in different cognitive functions. Significant connectivity with the left AI seed was observed for various brain regions in all three approaches at $p < 0.05$ (corrected for multiple comparisons). Highest connectivity was in all cases observed for the vicinity of the left AI seed extending into the surrounding inferior frontal cortex as well as for its right homotope and the (pre-) supplementary motor area (SMA; Fig. 2).

Regions commonly connected to the AI in all three approaches were identified by a conjunction analysis across the RS, MACM and SC connectivity maps. Three converging clusters were identified by this conjunction (Fig. 3A and Table 1). Two of these were centered on the bilateral AI (on the left reaching into the putamen) extending into the IFG and the precentral gyrus. The third was localized in the posterior medial frontal cortex (SMA/pre-SMA).

The functional characterization of these regions that were shown to be coupled with the AI across all three approaches pointed to a strong association of these with language and speech-related processes including semantics, phonology and syntax. Additionally, an association to attention, working memory and action inhibition was revealed (Fig. 3B).

Pairwise conjunctions (Fig. 4A, C and E) and contrasts (Fig. 4B, D and F) of these three connectivity maps indicated both commonalities of and differences between the three approaches to functional connectivity. We thus assessed the specific AI connectivity revealed by each of the three methods compared to the two other ones by computing the conjunction across each pair of contrasts displayed in Fig. 4B, D and F. Note that as strong local ispilateral and contralateral AI connectivity was revealed by all approaches, the AI was unsurprisingly not revealed to be a part of any of these specific networks.

Specific RS connectivity of the AI, i.e., RS connectivity that was significantly stronger than the connectivity revealed by MACM and SC analysis, was observed in the bilateral superior temporal gyrus (STG)/ posterior insula (extending on the left into the parietal operculum), ventrolateral prefrontal cortex (VLPFC), inferior parietal cortex (IPC), V1/V2, anterior midcingulate cortex (aMCC), SMA, putamen and left precentral gyrus. Specific MACM connectivity was observed in the bilateral fusiform gyrus/cerebellum and in the right IPC. Specific SC with the AI was found bilaterally in the ventromedial (VMPFC), dorsomedial (DMPFC) and dorsolateral prefrontal cortex (DLPFC), in the middle temporal gyrus (MTG), posterior cingulate cortex (PCC), in the right

Please cite this article as: Clos, M., et al., Comparison of structural covariance with functional connectivity approaches exemplified by an investigation of the left anterior i..., NeuroImage (2014), http://dx.doi.org/10.1016/j.neuroimage.2014.05.030

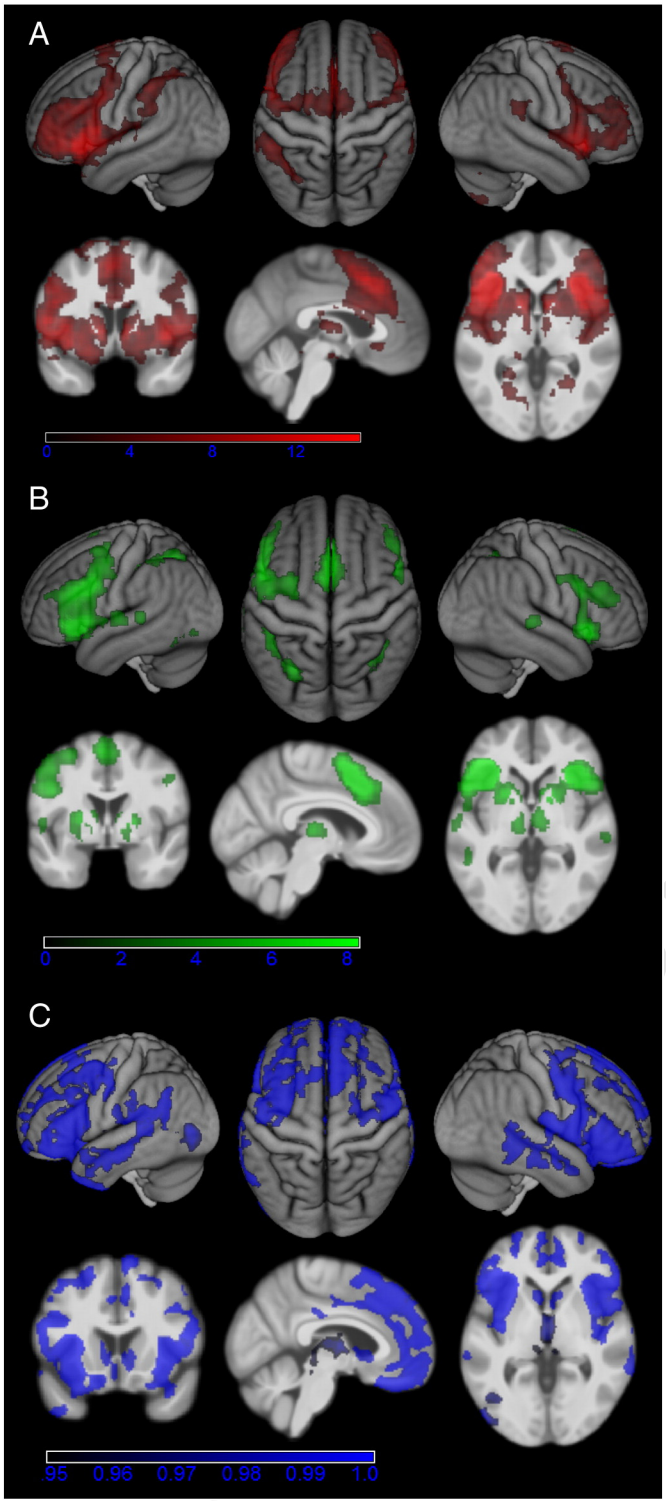

Fig. 2. Connectivity of the left anterior insula seed. (A) Regions showing significant resting state connectivity with the left anterior insula seed (cluster-level FWE-corrected at $p < 0.05$). (B) Regions showing significant MACM connectivity with the left anterior insula seed (cluster-level FWE-corrected $p < 0.05$). (C) Regions showing significant structural covariance with the anterior insula seed (TFCE-corrected at $p < 0.05$).

ventrolateral prefrontal cortex (VLPFC), right hippocampus/amygdala, left temporal pole and left angular gyrus (AG; Fig. 5A and Table 2).

Subsequently, these specific networks were likewise functionally characterized using the BrainMap meta-data. The regions specifically revealed by RS connectivity were primarily associated with auditory perception (including music), cognition, pain perception and reward. The regions specifically connected to the AI in the MACM analysis were significantly associated with several cognitive processes including vision and spatial processing but also with more language-related processes such as phonology, orthography, semantics and working memory. Finally, the regions specifically highlighted as connected to the AI by the structural covariance were mainly associated with emotion, social cognition, reward and memory (Fig. 5B).

Discussion

The aim of the current study was to delineate the function of a left anterior insula (AI) region and to compare structural covariance with task-free and task-based functional connectivity of this particular region. The choice of this left AI region as a seed for the connectivity analyses was motivated by its central role in working memory in healthy participants (Rottschy et al., 2012) and by findings of atrophy in patients with schizophrenia in this region (Nickl-Jockschat et al., 2011). Using the left AI as a seed thus allowed us to compare the three connectivity mapping approaches for a region involved in a key component of cognitive functioning in healthy subjects and affected by a highly prevalent mental disorder. Moreover, the high base rate of activation across many different tasks reported for the anterior insula (Chang et al., 2013; Yarkoni et al., 2011) and neuropsychological lesion evidence (Jones et al., 2010) indicates that this region contributes to a large variety of functional networks. This presumed broad functional involvement makes the anterior insula an ideal target to investigate differences between connectivity approaches as specific networks might preferably be revealed by the different approaches. Thus, the rather little functional specialization of the left AI should increase the chance of establishing a (potential) link between a method and the functional networks that it is biased to.

Converging AI connectivity

Importantly, all three connectivity approaches converged on a network comprising the right AI homotope, the bilateral inferior frontal gyrus (IFG), precentral gyrus, supplementary motor area (SMA) as well as the left putamen. This finding, in combination with previous reports that RS and SC yield similar connectivity patterns (He et al., 2007; Seeley et al., 2009), thus supports the assumption that covariance of gray matter volume reflects functional networks in the brain. Extending previous comparisons of SC and task-free RS functional connectivity measured in the same sample of participants, the current study furthermore demonstrated convergence with task-based MACM functional connectivity computed across many experiments and subject samples. We have thus verified that common networks may be revealed across highly divergent methods. Moreover, the characterization of this common network indicated a primary role in language processes including semantics, phonology, syntax, overt speech and reading. Although other processes such as working memory, attention, action inhibition, visual and gustatory perception were linked with this network as well, the relative dominance of language processes indicated that the common denominator of this consistently revealed network is language. This dominance of language processes is in agreement with meta-analytic findings showing that language-related processes preferentially activate the anterior–dorsal part of the insula (Mutschler et al., 2009) and with studies linking AI activation with lexico-semantic (Crepaldi et al., 2013; Vigneau et al., 2011) as well as with orthographic processing (Montant et al., 2011). However, it is peculiar that this convergent AI network does not feature typical temporal and parietal regions associated with language processing such as the STG/MTG and AG. Moreover, the language-characteristic lateralization towards the left is only observed for the putamen. Of note, temporal and left parietal regions are present in the structural covariance network but not in the resting state nor in the MACM network. Therefore, parts of the typical language network are also missing in the convergent network. However, the link of this convergent network with semantic, phonological and syntactic

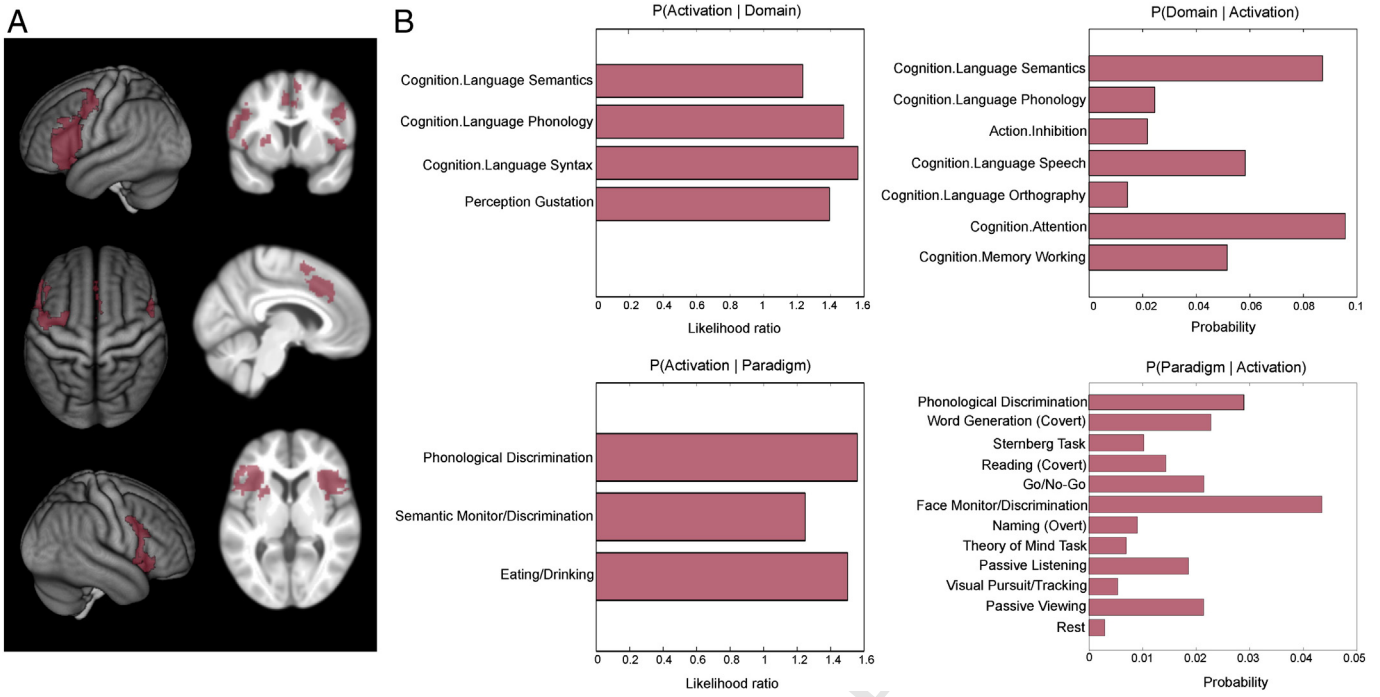

Fig. 3. Conjunction analysis of the left anterior insula and functional characterization. (A) Conjunction across resting state connectivity, MACM connectivity and structural covariance (additional cluster extent threshold of 100 voxels). (B) Functional characterization of the commonly connected regions based on the behavioral domain and paradigm class meta-data of the BrainMap database. All terms shown are significantly associated with the regions shown in (A) at $p < 0.05$ (FDR-corrected for multiple comparisons).

processes resulted directly from the quantitative reverse inference employed in the functional characterization and thus is not merely a subjective interpretation. Hence, the IFG, SMA, precentral gyrus and left putamen seem to share a common involvement in language processes, although they might not represent the complete language network. It is also possible that only a certain sub-function of these language processes might be the common denominator of this convergent AI network. Given that the functional characterization indicated working memory and attention mechanisms as additional domains of the convergent AI network, verbal working memory might be a prime candidate for a common function of these regions. Moreover, all these regions are known to be involved in motor control and could thus reflect predominant implication in speech articulation processes (Brown et al., 2009; Eickhoff et al., 2009a). Indeed the AI has been proposed to play a central role in the articulation of speech (Ackermann and Riecker, 2004).

Networks specifically associated with the individual connectivity approaches

Despite this common connectivity observed across all three approaches, striking differences were also found when contrasting the connectivity networks of the three techniques. In particular, specific RS functional connectivity of the left AI (compared to MACM and SC) highlighted the bilateral superior temporal gyrus, visual cortex, posterior insula, ventrolateral prefrontal cortex (VLPFC), inferior parietal cortex (IPC), SMA, anterior midcingulate cortex (aMCC), basal ganglia and the left precentral gyrus. These regions were found to be related with cognition, auditory perception, pain perception, reward as well as monitoring and discrimination in various sensory domains. The revealed connectivity pattern is highly similar to previous RS investigations of the (dorsal) AI reporting significant RS correlations in frontal, anterior cingulate, parietal and subcortical regions (Cauda et al., 2011; Chang et al., 2013; Deen et al., 2011). In contrast, specific MACM results highlighted language and covert speech processes as well as visual/spatial perception and working memory processes involving the fusiform gyrus and the cerebellum bilaterally as well as the right IPC. This specific MACM pattern deviates from previous findings based on meta-analytic co-activation of the dorsal AI using the Neurosynth framework rather than the BrainMap database (Chang et al., 2013). It may be noted that these authors also reported a very similar network as found with RS functional connectivity; however, connectivity patterns were

Table 1
Conjunction of AI connectivity.

Region	x	y	z	Cluster overlap with cytoarchitectonic area	Cluster size
Cluster 1				Area 44 (15%), 45 (8%), 6 (4%)	3134
L anterior insula	−35	20	−5		
L inferior frontal gyrus	−52	22	20		
L precentral gyrus	−46	1	43		
L putamen	−26	11	1		
Cluster 2				Area 44 (14%), 45 (6%)	1818
R anterior insula	37	22	3		
R inferior frontal gyrus	50	14	14		
R precentral gyrus	50	6	36		
Cluster 3				Area 6 (11%)	1153
Supplementary motor area	6	14	60		
Anterior cingulate cortex	−4	36	28		

x, *y*, and *z* coordinates refer to the peak voxel in MNI space. R, right; L, left.

Please cite this article as: Clos, M., et al., Comparison of structural covariance with functional connectivity approaches exemplified by an investigation of the left anterior i..., NeuroImage (2014), http://dx.doi.org/10.1016/j.neuroimage.2014.05.030

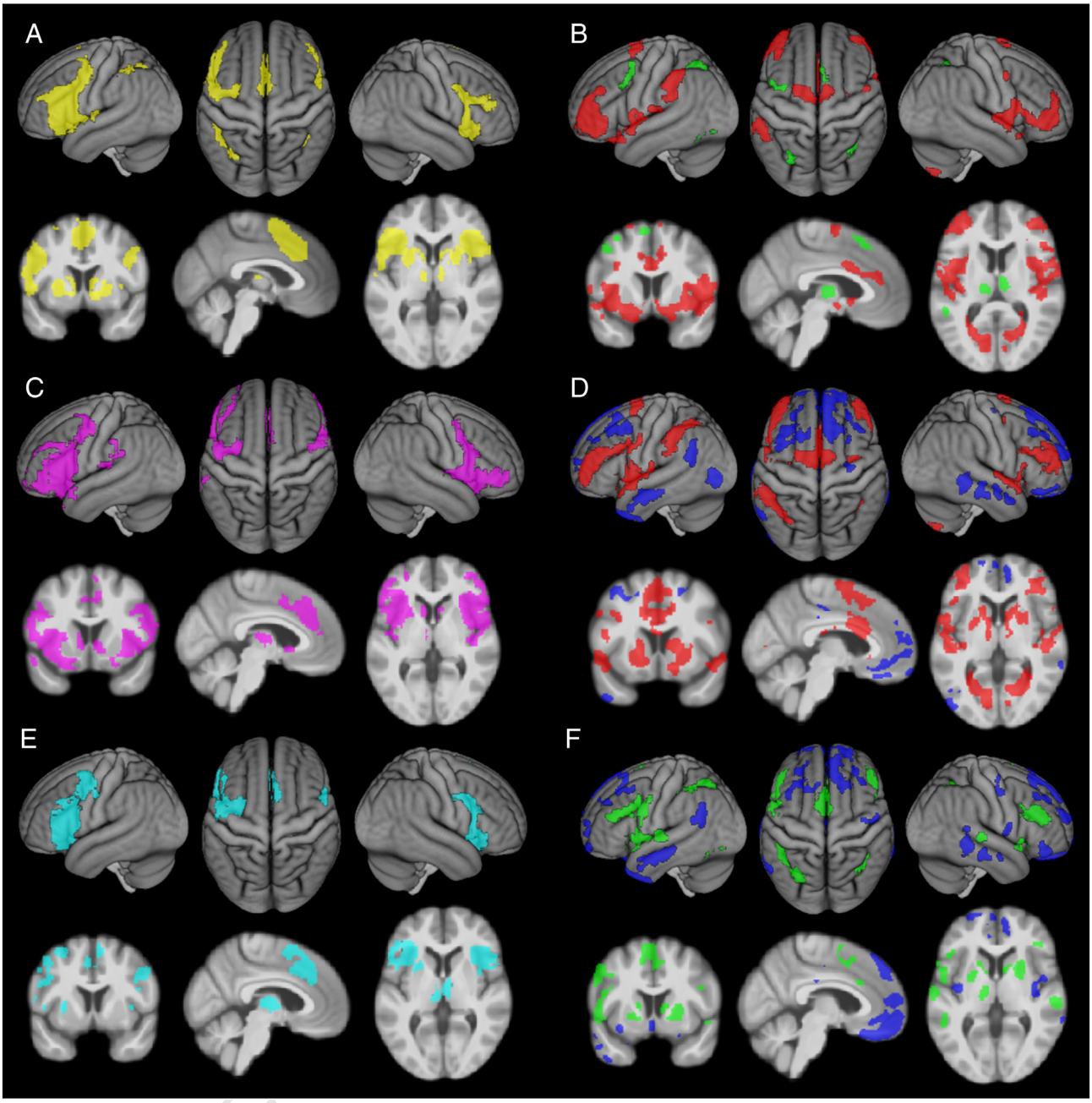

Fig. 4. Pairwise comparisons of the different connectivity measures of the left anterior insula. (A) Conjunction (yellow) and (B) contrast of resting state connectivity (red) and MACM connectivity (green). (C) Conjunction (violet) and (D) contrast of resting state connectivity (red) and structural covariance (blue). (E) Conjunction (cyan) and (F) contrast of MACM connectivity (green) and structural covariance (blue). An additional cluster extent threshold of 100 voxels is applied.

not explicitly contrasted in the previous analyses. Thus, the differences between the connectivity approaches are likely not that obvious and hence only revealed when directly comparing the resulting networks.

It may be argued that these diverging connectivity patterns are at least in part attributable to the conceptual differences of the functional connectivity approaches and, more specifically, the mental state of the subjects. RS functional connectivity is based on correlation of fMRI time-series measured under resting conditions, that is, it represents intrinsic synchronized activity that emerges in the absence of external stimulation (Deco and Corbetta, 2011; Fox and Raichle, 2007). Therefore, RS functional connectivity might tend to reveal networks of regions involved in the internal generation of events such as spontaneous cognition but also in the monitoring of internal needs and goals (Doucet et al., 2011; Jakobs et al., 2012; Schilbach et al., 2012) required for pain perception, reward processing as well as for discrimination processes in auditory and other sensory modalities. We would thus argue that the specific RS connectivity pattern reflects interactions of the seed during undirected attention covering both the internal milieu and external environment. In contrast, MACM represents conjoint, robust activation in response to exogenously controlled events and thus will most likely fail to reveal connectivity underlying internally initiated, spontaneous behavior and cognition (Eickhoff and Grefkes, 2011). Rather, MACM should mainly delineate regions that interact with the seed during the performance of structured tasks involving the maintenance of previously given task-set, the processing of sensory stimuli according to specified rules and the selection of a response from a predefined set. Therefore, the divergent functional connectivity patterns of the left AI associated with internal cognition and active perceptual and language processes might very well reflect the resting vs. active task state used for evaluating RS and MACM functional connectivity, respectively.

Please cite this article as: Clos, M., et al., Comparison of structural covariance with functional connectivity approaches exemplified by an investigation of the left anterior i..., NeuroImage (2014), http://dx.doi.org/10.1016/j.neuroimage.2014.05.030

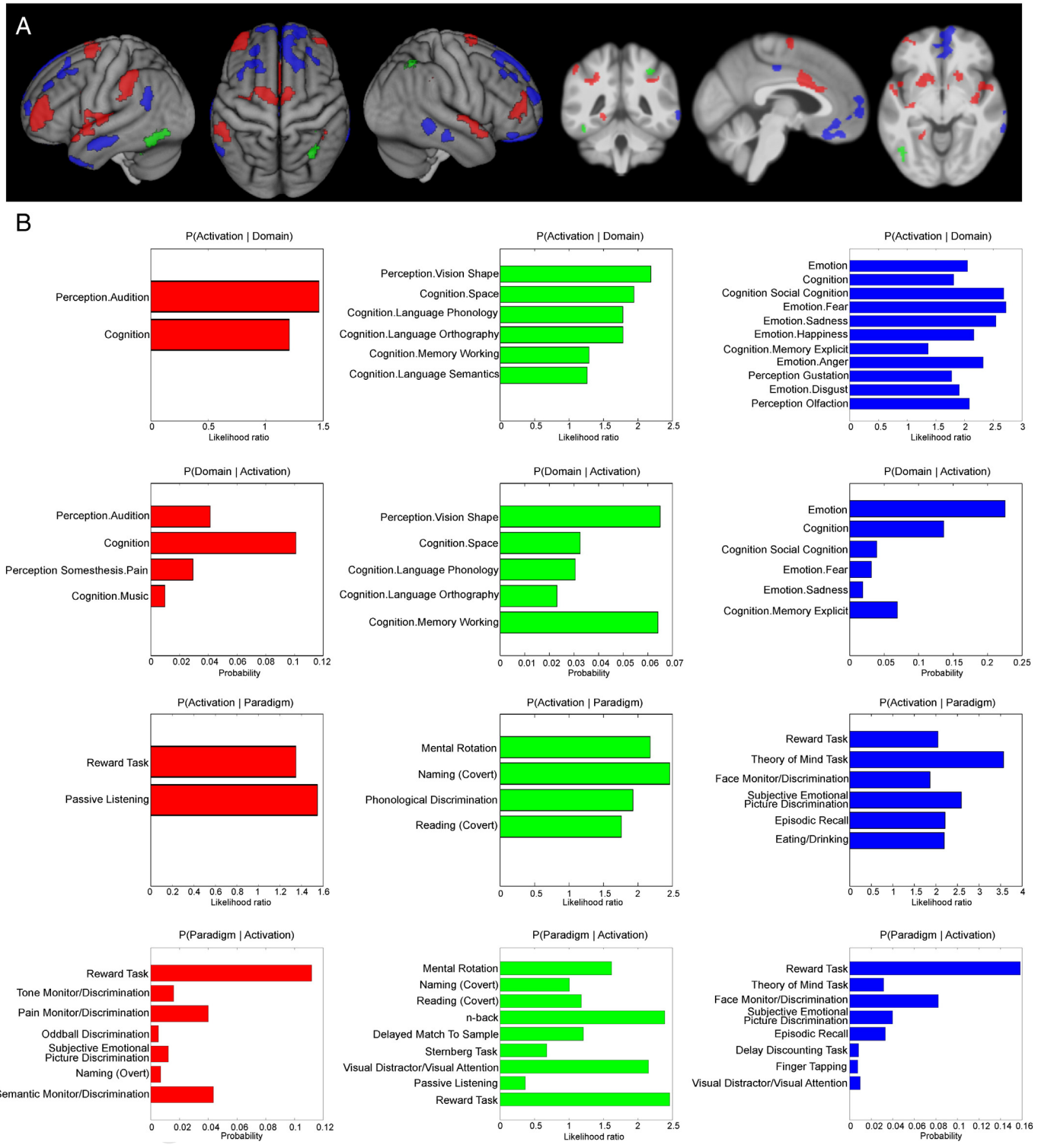

Fig. 5. Specific connectivity of the left anterior insula and functional characterization. (A) Specific contrasts between resting state connectivity (red), MACM connectivity (green) and structural covariance (blue). An additional cluster extent threshold of 100 voxels is applied. (B) Functional characterization of the specifically connected regions based on the behavioral domain and paradigm class meta-data of the BrainMap database. All terms shown are significantly associated with specific resting state connectivity (red), specific MACM connectivity (green) and specific structural covariance (blue) of the anterior insula at $p < 0.05$, respectively (FDR-corrected for multiple comparisons).

In contrast to the above mentioned functional connectivity approaches, structural covariance revealed an extensive network specifically devoted to (negative) emotions, social cognition, reward and explicit memory composed of ventromedial (VMPFC), dorsomedial (DMPFC) and dorsolateral prefrontal cortex (DLPFC), the middle temporal gyrus (MTG), posterior cingulate cortex (PCC), the right ventrolateral prefrontal cortex (VLPFC), right hippocampus/amygdala, left temporal pole and left angular gyrus. Firstly, it should be stressed that this network shows a strong functional relation despite the fact that it was defined by anatomical covariance. In combination with the conjunction results across structural and functional connectivity, this again emphasizes that SC should reflect functionally specific brain networks. However, it may be noted that the specific SC network showed a striking association with social cognition and (mainly negative) emotional processing compared to the

Table 2
Specific AI connectivity.

Region	x	y	z	Cluster overlap with cytoarchitectonic area	Cluster size
RS					
L STG/posterior insula/ parietal operculum	−46	−9	1	TE 1.0 (13%), TE 1.2 (4%), OP4 (12%), Ig2 (7%)	742
L VLPFC	−36	48	6		738
L IPL	−47	−40	38	PF (42%), hIP1 (17%), PFcm (9%), hIP2 (6%)	643
L V1/V2	−18	−66	4	Area 17 (61%), 18 (11%)	564
L putamen	−17	6	−5		285
L precentral gyrus	−33	−3	41	Area 6 (2%)	206
R STG/posterior insula	47	−6	−4	TE 1.1 (13%), TE 1.0 (12%), TE 1.2 (10%), Id1 (3%)	567
R V1/V2	22	−63	5	Area 17 (85%), 18 (7%)	338
R VLPFC	39	45	8		292
R putamen	15	11	−11		263
R IPL	39	−45	38	hIP1 (42%), hIP3 (11%), PF (6%), hIP2 (4%)	162
MCC	1	12	29		448
SMA	−5	−4	67	Area 6 (96%)	386
MACM					
L fusiform gyrus/cerebellum	−39	−61	−18		746
R fusiform gyrus/cerebellum	32	−64	−21		180
R IPL	33	54	49	hIP3 (64%)	169
SC					
L MTG	−62	−12	−17		460
L temporal pole	−42	11	−39		120
L DLPFC	−25	24	49		353
L AG	−58	−57	26	PGa (50%), PFm (29%)	247
R DMPFC	12	39	47		973
R hippocampus/amygdala	20	−5	−26	EC (58%), SUB (4%), LB (20%)	259
R MTG	66	−42	−4		218
R VLPFC	43	39	−17		125
R DLPFC	33	36	40		118
R MTG	68	−24	−14		101
VMPFC	4	48	−7		4348
PCC	−1	−25	42		155

x, *y*, and *z* coordinates refer to the centre of gravity in MNI space. R, right; L, left.

functional connectivity networks. That is, whereas RS and MACM revealed predominantly perceptual and language networks, this was not the case for SC. The strong dominance of social cognition is particular remarkable as the functional characterization of the left AI seed region as well as the conjunction network across connectivity approaches did not indicate a specific involvement of the left AI in social processing. However, a central role for the AI in aspects of social cognition processes including empathy (Singer et al., 2004, 2009) is widely recognized. It is thus not the association of social–emotional processes with left AI per se, but rather the exclusive reflection of these processes in the SC network that may be surprising. In support of the validity of our SC results, the current network strongly resembles a previously reported SC pattern of a left AI seed with several regions that clearly stood out in the current SC analysis including the VMPFC, DMPFC, VLPFC, DLPFC, as well as the lateral and medial temporal cortex (Bernhardt et al., 2013). Furthermore, this earlier study showed that the SC between VLPFC and the left AI correlated positively with empathy. Thus, the current SC findings of the left AI are well in line with a previously detected SC network of the left AI and a proposed role of this network in social cognition.

Still, the question remains why this "social" network is so much more dominant in SC as compared to the other functional connectivity approaches. While the exact biological basis of SC is still rather unclear, SC networks have been hypothesized to arise from mutual trophic effects mediated by axonal connections and experience-related plasticity affecting regions within a functional network similarly (Evans, 2013; Mechelli et al., 2005) in addition to genetic factors determining brain morphology (Thompson et al., 2001). The SC pattern of the left AI might thus reflect dominant long-term synchronized developmental patterns within the social cognition network, which could indicate that the brain is literally wired for social interactions, as also proposed by the social brain hypothesis (Dunbar, 2009; Dunbar and Shultz, 2007; Insel and Fernald, 2004). Importantly, these would represent relatively "slow" processes continuously shaping the brain over years and decades. Approaches to task-based (MACM) and task-free (RS) functional connectivity on the other hand might rather highlight more flexibly employed functional network interactions. Therefore, they would pick up the transients of brain connectivity in a particular context (mind-wandering or experimental tasks) but much less such anatomically imprinted long-term interactions in a complex (social) world. This would imply that also other forms of anatomical connectivity of the AI should primarily reveal regions involved in social–emotional processes. Indeed there is some evidence for this, as anatomical tracer studies in monkeys found strong reciprocal interconnectivity between the AI and various limbic regions including the orbitofrontal cortex, temporal pole and amygdala (Mesulam and Mufson, 1982; Mufson and Mesulam, 1982). Noninvasive diffusion imaging of the human insula similarly identified anatomical connections the AI with orbitofrontal, temporal, and inferior frontal regions (Cloutman et al., 2012; Jakab et al., 2012) as well as with the amygdala (Cerliani et al., 2012). While these studies did not observe particular anatomical connectivity between the AI and midline regions that was prominent in our SC pattern, remarkably strong anatomical connectivity (but no RS functional connectivity) between the insula and medial frontal gyrus as well as the PCC was reported by Skudlarski et al. (2008). Of interest, most diffusion-based anatomical connectivity studies unequivocally report lack of anatomical connectivity between the insula and the ACC in humans (Beckmann et al., 2009; Cerliani et al., 2012; Cloutman et al., 2012), which is in sharp contrast to functional connectivity findings (Cauda et al., 2011; Taylor et al., 2009). And indeed, despite the striking covariance between the AI and midline structures in the current study, the ACC seemed to be spared in both the specific and the non-specific SC pattern. These results thus imply that connectivity between the ACC and the insula is not captured by noninvasive connectivity methods based on anatomical characteristics.

Please cite this article as: Clos, M., et al., Comparison of structural covariance with functional connectivity approaches exemplified by an investigation of the left anterior i..., NeuroImage (2014), http://dx.doi.org/10.1016/j.neuroimage.2014.05.030

In spite of the plausible hypotheses stated above, the small number of previously performed comparisons between SC approaches and functional connectivity in addition to the uncertainties regarding the biological basis of SC do not allow us to derive ultimate conclusions from the current study. Future studies comparing SC with functional connectivity approaches using other seed regions will be needed in order to establish whether SC indeed preferably reveals certain presumably hard-wired networks such as social cognition and emotion networks and to what extent this pattern might depend on the seed region. Also, a better understanding of the biological processes driving SC would help with the interpretation of the specific functional implication reflected in the SC networks. Moreover, it is important to acknowledge that, in addition to the conceptual differences of the three connectivity approaches, unequal noise effects might also contribute to diverging connectivity patterns. That is, noise and measurement error may vary across the connectivity approaches (Eickhoff et al., 2011). For example, MACM is very vulnerable to variability in the location of activations reported across studies due to limited sample sizes and different templates used for normalization of imaging data (Eickhoff et al., 2009b), while RS fluctuations can be confounded by low-frequency physiological signals and movement (Bandettini and Bullmore, 2008; Fox et al., 2009) whose impact furthermore varies across brain regions (Skudlarski et al., 2008). For SC on the other hand, the accuracy of the segmentation of the brain tissue might differ across the cortex and distort connectivity results (Lerch et al., 2006).

Still, such biases in measurement noise fail to explain the clear differences in network characterization that point to specific functional roles in internal cognition for RS, active cognition and perception in MACM and social cognition in SC. In particular, the properties of the RS and MACM networks are well in accordance with what would be expected based on their conceptual differences in a resting and an active task setting, respectively. Likewise, long-term maturational effects in the brain reflecting the importance of social interactions could explain the preferential delineation of social cognition-related areas by SC analysis.

Role of the left AI in health and disease

The non-significance of the FDR-corrected functional characterization of the left AI indicated a high base rate of activation across many different tasks and thus little functional specialization in this region. This is in agreement with proposals of the anterior insula as an integrative region involved in multiple functions (Craig, 2009; Dosenbach et al., 2006; Kurth et al., 2010). Still, the uncorrected functional characterization results demonstrate that language, memory and emotion processes seem to dominate in this portion of the anterior insula. These findings are in accordance with the two meta-analyses that served to define the AI seed region. In this context, we would like to highlight that such accordance is not trivial or circular, as the previous analyses were not based on the BrainMap database. Firstly, the results reflect the importance of the left AI seed in working memory observed in the meta-analysis by (Rottschy et al., 2012). In particular, this previous meta-analysis found the left AI to be part of a network involved in working memory independently of the type of stimuli and task which might thus qualify as the central executive network of the brain. Secondly, the characterization results converge with the findings of gray matter atrophy in this region in schizophrenia (Nickl-Jockschat et al., 2011). Schizophrenia is associated with symptoms in the language domain [e.g. auditory verbal hallucinations (Jardri et al., 2011; Seal et al., 2004), but also with disorganized speech and alogia (Becker et al., 2012; DeLisi, 2001)], socio-emotional disturbances [e.g. flattened affect (Gur et al., 2006; Kirkpatrick et al., 2001) and social cognition deficits (Savla et al., 2013)] as well as working memory and executive function impairments (Dibben et al., 2009; Glahn et al., 2005; Lee and Park, 2005; Minzenberg et al., 2009). Given the interaction patterns revealed in the current study, we would suggest that a considerable amount of the symptoms displayed by schizophrenic patients might involve the left AI and the networks connected to it.

Indeed, neuroimaging studies have pointed to abnormal insular involvement in schizophrenic symptoms including auditory–verbal hallucinations (Clos et al., 2014; Dierks et al., 1999; Hoffman et al., 2008; Shergill et al., 2000; Sommer et al., 2008), impairment of verbal fluency (Curtis et al., 1998), working memory (Glahn et al., 2005; Hashimoto et al., 2010) and emotions (Crespo-Facorro et al., 2001; Lee et al., 2014; Phillips et al., 1999; Seiferth et al., 2009). Previous proposals of insular dysfunction in schizophrenia have mainly focused on its role in distinguishing internal and external sensory events (Crespo-Facorro et al., 2000; Wylie and Tregellas, 2010) and salience (Menon and Uddin, 2010). While these accounts could explain how hallucinations and other disturbed perceptions could arise from insular dysfunction, the connectivity patterns and the functional characterization of the left AI moreover suggest that also other symptoms including working memory impairments and socio-emotional deficits might result from insular dysfunction. Together with the structural abnormalities in the left AI (Nickl-Jockschat et al., 2011), the current findings thus indicate that abnormal functioning of the AI and its associated functional networks might lead to impaired integration within and between language, working memory and socio-emotional systems in schizophrenia. Moreover, with regard to healthy brain functioning, our results are in line with previous accounts proposing that the integration of internal and external events across multiple modalities into a coherent experience (Craig, 2009; Kurth et al., 2010; Sterzer and Kleinschmidt, 2010), salience detection (Menon and Uddin, 2010) or task-set maintenance (Dosenbach et al., 2006) could be the core function of this region. The current results emphasized the AI's role in various cognitive domains including language, working-memory and affect under both active task and resting state. Thus, the AI is involved in processes underlying spontaneous, internally generated cognition and action as well as behavior in response to exogenously controlled events. Moreover, social cognition heavily relies on the successful integration internal needs, emotions and goals with the demands of the environment. Therefore, the AI seems to be extremely suited to integrate perception, cognition, affect and action caused by internal and external events into a coherent whole. This interpretation in turn would be in accordance with the often suggested integrative role of the AI.

Finally, the comparison of the connectivity approaches points out that some functions of the left AI are differentially highlighted by different connectivity approaches. In particular, the association of RS functional connectivity with internal cognition, MACM functional connectivity with active perceptual and language processes and SC with social cognition stresses the importance of investigating multiple connectivity forms when trying to understand the contribution of certain brain regions as well as the brain networks underlying complex psychiatric disorders.

Acknowledgments

This work was supported by the National Institute of Mental Health (R01-MH074457), the Initiative and Networking Fund of the Helmholtz Association within the Helmholtz Alliance on Systems Biology (Human Brain Model SBE, MC), and the DFG (IRTG 1328 to SBE).

References

Ackermann, H., Riecker, A., 2004. The contribution of the insula to motor aspects of speech production: a review and a hypothesis. Brain Lang. 89, 320–328.
Albaugh, M.D., Ducharme, S., Collins, D.L., Botteron, K.N., Althoff, R.R., Evans, A.C., Karama, S., Hudziak, J.J., Brain Development Cooperative Group, 2013. Evidence for a cerebral cortical thickness network anti-correlated with amygdalar volume in healthy youths: implications for the neural substrates of emotion regulation. Neuroimage 71, 42–49.
Alexander-Bloch, A., Raznahan, A., Bullmore, E., Giedd, J., 2013. The convergence of maturational change and structural covariance in human cortical networks. J. Neurosci. 33, 2889–2899.
Andrews, T.J., Halpern, S.D., Purves, D., 1997. Correlated size variations in human visual cortex, lateral geniculate nucleus, and optic tract. J. Neurosci. 17, 2859–2868.
Ashburner, J., Friston, K.J., 2005. Unified segmentation. Neuroimage 26, 839–851.

Please cite this article as: Clos, M., et al., Comparison of structural covariance with functional connectivity approaches exemplified by an investigation of the left anterior i..., NeuroImage (2014), http://dx.doi.org/10.1016/j.neuroimage.2014.05.030

Bandettini, P.A., Bullmore, E., 2008. Endogenous oscillations and networks in functional magnetic resonance imaging. Hum. Brain Mapp. 29, 737–739.

Becker, T.M., Cicero, D.C., Cowan, N., Kerns, J.G., 2012. Cognitive control components and speech symptoms in people with schizophrenia. Psychiatry Res. 196, 20–26.

Beckmann, M., Johansen-Berg, H., Rushworth, M.F.S., 2009. Connectivity-based parcellation of human cingulate cortex and its relation to functional specialization. J. Neurosci. 29, 1175–1190.

Bernhardt, B.C., Worsley, K.J., Besson, P., Concha, L., Lerch, J.P., Evans, A.C., Bernasconi, N., 2008. Mapping limbic network organization in temporal lobe epilepsy using morphometric correlations: insights on the relation between mesiotemporal connectivity and cortical atrophy. Neuroimage 42, 515–524.

Bernhardt, B.C., Klimecki, O.M., Leiberg, S., Singer, T., 2013. Structural covariance networks of the dorsal anterior insula predict females' individual differences in empathic responding. Cereb. Cortex. http://dx.doi.org/10.1093/cercor/bht072 (Advance online publication).

Biswal, B., Yetkin, F.Z., Haughton, V.M., Hyde, J.S., 1995. Functional connectivity in the motor cortex of resting human brain using echo-planar MRI. Magn. Reson. Med. 34, 537–541.

Brown, S., Laird, A.R., Pfordresher, P.Q., Thelen, S.M., Turkeltaub, P., Liotti, M., 2009. The somatotopy of speech: phonation and articulation in the human motor cortex. Brain Cogn. 70, 31–41.

Bullmore, E.T., Woodruff, P.W., Wright, I.C., Rabe-Hesketh, S., Howard, R.J., Shuriquie, N., Murray, R.M., 1998. Does dysplasia cause anatomical dysconnectivity in schizophrenia? Schizophr. Res. 30, 127–135.

Cauda, F., Cavanna, A.E., D'agata, F., Sacco, K., Duca, S., Geminiani, G.C., 2011. Functional connectivity and coactivation of the nucleus accumbens: a combined functional connectivity and structure-based meta-analysis. J. Cogn. Neurosci. 23, 2864–2877.

Cerliani, L., Thomas, R.M., Jbabdi, S., Siero, J.C.W., Nanetti, L., Crippa, A., Gazzola, V., D'Arceuil, H., Keysers, C., 2012. Probabilistic tractography recovers a rostrocaudal trajectory of connectivity variability in the human insular cortex. Hum. Brain Mapp. 33, 2005–2034.

Chang, L.J., Yarkoni, T., Khaw, M.W., Sanfey, A.G., 2013. Decoding the role of the insula in human cognition: functional parcellation and large-scale reverse inference. Cereb. Cortex 23, 739–749.

Clos, M., Diederen, K.M.J., Meijering, A.L., Sommer, I.E., Eickhoff, S.B., 2014. Aberrant connectivity of areas for decoding degraded speech in patients with auditory verbal hallucinations. Brain Struct. Funct. 219, 581–594.

Cloutman, L.L., Binney, R.J., Drakesmith, M., Parker, G.J.M., Lambon Ralph, M.A., 2012. The variation of function across the human insula mirrors its patterns of structural connectivity: evidence from in vivo probabilistic tractography. Neuroimage 59, 3514–3521.

Craig, A.D.B., 2009. How do you feel–now? The anterior insula and human awareness. Nat. Rev. Neurosci. 10, 59–70.

Crepaldi, D., Berlingeri, M., Cattinelli, I., Borghese, N.A., Luzzatti, C., Paulesu, E., 2013. Clustering the lexicon in the brain: a meta-analysis of the neurofunctional evidence on noun and verb processing. Front. Hum. Neurosci. 7, 303.

Crespo-Facorro, B., Kim, J., Andreasen, N.C., O'Leary, D.S., Bockholt, H.J., Magnotta, V., 2000. Insular cortex abnormalities in schizophrenia: a structural magnetic resonance imaging study of first-episode patients. Schizophr. Res. 46, 35–43.

Crespo-Facorro, B., Paradiso, S., Andreasen, N.C., O'Leary, D.S., Watkins, G.L., Ponto, L.L., Hichwa, R.D., 2001. Neural mechanisms of anhedonia in schizophrenia: a PET study of response to unpleasant and pleasant odors. JAMA 286, 427–435.

Curtis, V.A., Bullmore, E.T., Brammer, M.J., Wright, I.C., Williams, S.C., Morris, R.G., Sharma, T.S., Murray, R.M., McGuire, P.K., 1998. Attenuated frontal activation during a verbal fluency task in patients with schizophrenia. Am. J. Psychiatry 155, 1056–1063.

Deco, G., Corbetta, M., 2011. The dynamical balance of the brain at rest. Neuroscientist 17, 107–123.

Deen, B., Pitskel, N.B., Pelphrey, K.A., 2011. Three systems of insular functional connectivity identified with cluster analysis. Cereb. Cortex 21, 1498–1506.

DeLisi, L.E., 2001. Speech disorder in schizophrenia: review of the literature and exploration of its relation to the uniquely human capacity for language. Schizophr. Bull. 27, 481–496.

Dibben, C.R.M., Rice, C., Laws, K., McKenna, P.J., 2009. Is executive impairment associated with schizophrenic syndromes? A meta-analysis. Psychol. Med. 39, 381–392.

Dierks, T., Linden, D.E., Jandl, M., Formisano, E., Goebel, R., Lanfermann, H., Singer, W., 1999. Activation of Heschl's gyrus during auditory hallucinations. Neuron 22, 615–621.

Dosenbach, N.U.F., Visscher, K.M., Palmer, E.D., Miezin, F.M., Wenger, K.K., Kang, H.C., Burgund, E.D., Grimes, A.L., Schlaggar, B.L., Petersen, S.E., 2006. A core system for the implementation of task sets. Neuron 50, 799–812.

Doucet, G., Naveau, M., Petit, L., Delcroix, N., Zago, L., Crivello, F., Jobard, G., Tzourio-Mazoyer, N., Mazoyer, B., Mellet, E., Joliot, M., 2011. Brain activity at rest: a multiscale hierarchical functional organization. J. Neurophysiol. 105, 2753–2763.

Draganski, B., Gaser, C., Busch, V., Schuierer, G., Bogdahn, U., May, A., 2004. Neuroplasticity: changes in grey matter induced by training. Nature 427, 311–312.

Driemeyer, J., Boyke, J., Gaser, C., Büchel, C., May, A., 2008. Changes in gray matter induced by learning–revisited. PLoS One 3, e2669.

Dunbar, R.I.M., 2009. The social brain hypothesis and its implications for social evolution. Ann. Hum. Biol. 36, 562–572.

Dunbar, R.I.M., Shultz, S., 2007. Evolution in the social brain. Science 317, 1344–1347.

Eickhoff, S.B., Grefkes, C., 2011. Approaches for the integrated analysis of structure, function and connectivity of the human brain. Clin. EEG Neurosci. 42, 107–121.

Eickhoff, S.B., Heim, S., Zilles, K., Amunts, K., 2009a. A systems perspective on the effective connectivity of overt speech production. Philos. Transact. A Math. Phys. Eng. Sci. 367, 2399–2421.

Eickhoff, S.B., Laird, A.R., Grefkes, C., Wang, L.E., Zilles, K., Fox, P.T., 2009b. Coordinate-based activation likelihood estimation meta-analysis of neuroimaging data: a random-effects approach based on empirical estimates of spatial uncertainty. Hum. Brain Mapp. 30, 2907–2926.

Eickhoff, S.B., Jbabdi, S., Caspers, S., Laird, A.R., Fox, P.T., Zilles, K., Behrens, T.E.J., 2010. Anatomical and functional connectivity of cytoarchitectonic areas within the human parietal operculum. J. Neurosci. 30, 6409–6421.

Eickhoff, S.B., Bzdok, D., Laird, A.R., Roski, C., Caspers, S., Zilles, K., Fox, P.T., 2011. Co-activation patterns distinguish cortical modules, their connectivity and functional differentiation. Neuroimage 57, 938–949.

Eickhoff, S.B., Bzdok, D., Laird, A.R., Kurth, F., Fox, P.T., 2012. Activation likelihood estimation meta-analysis revisited. Neuroimage 59, 2349–2361.

Evans, A.C., 2013. Networks of anatomical covariance. Neuroimage 80, 489–504.

Fox, P.T., Lancaster, J.L., 2002. Opinion: mapping context and content: the BrainMap model. Nat. Rev. Neurosci. 3, 319–321.

Fox, M.D., Raichle, M.E., 2007. Spontaneous fluctuations in brain activity observed with functional magnetic resonance imaging. Nat. Rev. Neurosci. 8, 700–711.

Fox, M.D., Zhang, D., Snyder, A.Z., Raichle, M.E., 2009. The global signal and observed anticorrelated resting state brain networks. J. Neurophysiol. 101, 3270–3283.

Glahn, D.C., Ragland, J.D., Abramoff, A., Barrett, J., Laird, A.R., Bearden, C.E., Velligan, D.I., 2005. Beyond hypofrontality: a quantitative meta-analysis of functional neuroimaging studies of working memory in schizophrenia. Hum. Brain Mapp. 25, 60–69.

Gur, R.E., Kohler, C.G., Ragland, J.D., Siegel, S.J., Lesko, K., Bilker, W.B., Gur, R.C., 2006. Flat affect in schizophrenia: relation to emotion processing and neurocognitive measures. Schizophr. Bull. 32, 279–287.

Haier, R.J., Karama, S., Leyba, L., Jung, R.E., 2009. MRI assessment of cortical thickness and functional activity changes in adolescent girls following three months of practice on a visual-spatial task. BMC Res. Notes 2, 174.

Hashimoto, R., Lee, K., Preus, A., McCarley, R.W., Wible, C.G., 2010. An fMRI study of functional abnormalities in the verbal working memory system and the relationship to clinical symptoms in chronic schizophrenia. Cereb. Cortex 20, 46–60.

He, Y., Chen, Z.J., Evans, A.C., 2007. Small-world anatomical networks in the human brain revealed by cortical thickness from MRI. Cereb. Cortex 17, 2407–2419. http://dx.doi.org/10.1093/cercor/bhl149.

Hoffman, R.E., Anderson, A.W., Varanko, M., Gore, J.C., Hampson, M., 2008. Time course of regional brain activation associated with onset of auditory/verbal hallucinations. Br. J. Psychiatry 193, 424–425.

Hoffstaedter, F., Grefkes, C., Caspers, S., Roski, C., Palomero-Gallagher, N., Laird, A.R., Fox, P. T., Eickhoff, S.B., 2014. The role of anterior midcingulate cortex in cognitive motor control: evidence from functional connectivity analyses. Hum. Brain Mapp. 35, 2741–2753.

Insel, T.R., Fernald, R.D., 2004. How the brain processes social information: searching for the social brain. Annu. Rev. Neurosci. 27, 697–722.

Jakab, A., Molnár, P.P., Bogner, P., Béres, M., Berényi, E.L., 2012. Connectivity-based parcellation reveals interhemispheric differences in the insula. Brain Topogr. 25, 264–271.

Jakobs, O., Langner, R., Caspers, S., Roski, C., Cieslik, E.C., Zilles, K., Laird, A.R., Fox, P.T., Eickhoff, S.B., 2012. Across-study and within-subject functional connectivity of a right temporo-parietal junction subregion involved in stimulus-context integration. Neuroimage 60, 2389–2398.

Jardri, R., Pouchet, A., Pins, D., Thomas, P., 2011. Cortical activations during auditory verbal hallucinations in schizophrenia: a coordinate-based meta-analysis. Am. J. Psychiatry 168, 73–81.

Jones, C.L., Ward, J., Critchley, H.D., 2010. The neuropsychological impact of insular cortex lesions. J. Neurol. Neurosurg. Psychiatry 81, 611–618.

Kelly, C., Toro, R., Di Martino, A., Cox, C.L., Bellec, P., Castellanos, F.X., Milham, M.P., 2012. A convergent functional architecture of the insula emerges across imaging modalities. Neuroimage 61, 1129–1142.

Kirkpatrick, B., Buchanan, R.W., Ross, D.E., Carpenter Jr., W.T., 2001. A separate disease within the syndrome of schizophrenia. Arch. Gen. Psychiatry 58, 165–171.

Kousta, S., 2013. Mapping the structural and functional architecture of the brain. Trends Cogn. Sci. 17, 595.

Kurth, F., Zilles, K., Fox, P.T., Laird, A.R., Eickhoff, S.B., 2010. A link between the systems: functional differentiation and integration within the human insula revealed by meta-analysis. Brain Struct. Funct. 214, 519–534.

Laird, A.R., Lancaster, J.L., Fox, P.T., 2005. BrainMap: the social evolution of a human brain mapping database. Neuroinformatics 3, 65–78.

Laird, A.R., Eickhoff, S.B., Kurth, F., Fox, P.M., Uecker, A.M., Turner, J.A., Robinson, J.L., Lancaster, J.L., Fox, P.T., 2009. ALE meta-analysis workflows via the Brainmap database: progress towards A probabilistic functional brain atlas. Front. Neuroinform. 3, 23.

Laird, A.R., Eickhoff, S.B., Fox, P.M., Uecker, A.M., Ray, K.L., Saenz Jr., J.J., McKay, D.R., Bzdok, D., Laird, R.W., Robinson, J.L., Turner, J.A., Turkeltaub, P.E., Lancaster, J.L., Fox, P.T., 2011. The BrainMap strategy for standardization, sharing, and meta-analysis of neuroimaging data. BMC Res. Notes 4, 349.

Laird, A.R., Eickhoff, S.B., Rottschy, C., Bzdok, D., Ray, K.L., Fox, P.T., 2013. Networks of task co-activations. Neuroimage 80, 505–514.

Lee, J., Park, S., 2005. Working memory impairments in schizophrenia: a meta-analysis. J. Abnorm. Psychol. 114, 599–611.

Lee, J.S., Chun, J.W., Yoon, S.Y., Park, H.-J., Kim, J.-J., 2014. Involvement of the mirror neuron system in blunted affect in schizophrenia. Schizophr. Res. 152, 268–274.

Lerch, J.P., Worsley, K., Shaw, W.P., Greenstein, D.K., Lenroot, R.K., Giedd, J., Evans, A.C., 2006. Mapping anatomical correlations across cerebral cortex (MACACC) using cortical thickness from MRI. Neuroimage 31, 993–1003.

Maguire, E.A., Spiers, H.J., Good, C.D., Hartley, T., Frackowiak, R.S.J., Burgess, N., 2003. Navigation expertise and the human hippocampus: a structural brain imaging analysis. Hippocampus 13, 250–259.

Please cite this article as: Clos, M., et al., Comparison of structural covariance with functional connectivity approaches exemplified by an investigation of the left anterior i..., NeuroImage (2014), http://dx.doi.org/10.1016/j.neuroimage.2014.05.030

Mechelli, A., Friston, K.J., Frackowiak, R.S., Price, C.J., 2005. Structural covariance in the human cortex. J. Neurosci. 25, 8303–8310.
Menon, V., Uddin, L.Q., 2010. Saliency, switching, attention and control: a network model of insula function. Brain Struct. Funct. 214, 655–667.
Mesulam, M.M., Mufson, E.J., 1982. Insula of the old world monkey. I. Architectonics in the insulo-orbito-temporal component of the paralimbic brain. J. Comp. Neurol. 212, 1–22.
Minzenberg, M.J., Laird, A.R., Thelen, S., Carter, C.S., Glahn, D.C., 2009. Meta-analysis of 41 functional neuroimaging studies of executive function in schizophrenia. Arch. Gen. Psychiatry 66, 811–822.
Mitelman, S.A., Brickman, A.M., Shihabuddin, L., Newmark, R., Chu, K.W., Buchsbaum, M.S. , 2005. Correlations between MRI-assessed volumes of the thalamus and cortical Brodmann's areas in schizophrenia. Schizophr. Res. 75, 265–281.
Montant, M., Schön, D., Anton, J.-L., Ziegler, J.C., 2011. Orthographic contamination of Broca's area. Front. Psychol. 2, 378.
Mufson, E.J., Mesulam, M.M., 1982. Insula of the old world monkey. II. Afferent cortical input and comments on the claustrum. J. Comp. Neurol. 212, 23–37.
Müller, V.I., Cieslik, E.C., Laird, A.R., Fox, P.T., Eickhoff, S.B., 2013. Dysregulated left inferior parietal activity in schizophrenia and depression: functional connectivity and characterization. Front. Hum. Neurosci. 7, 268.
Mutschler, I., Wieckhorst, B., Kowalevski, S., Derix, J., Wentlandt, J., Schulze-Bonhage, A., Ball, T., 2009. Functional organization of the human anterior insular cortex. Neurosci. Lett. 457, 66–70.
Nichols, T., Brett, M., Andersson, J., Wager, T., Poline, J.-B., 2005. Valid conjunction inference with the minimum statistic. Neuroimage 25, 653–660.
Nickl-Jockschat, T., Schneider, F., Pagel, A.D., Laird, A.R., Fox, P.T., Eickhoff, S.B., 2011. Progressive pathology is functionally linked to the domains of language and emotion: meta-analysis of brain structure changes in schizophrenia patients. Eur. Arch. Psychiatry Clin. Neurosci. 261 (Suppl. 2), S166–S171.
Phillips, M.L., Williams, L., Senior, C., Bullmore, E.T., Brammer, M.J., Andrew, C., Williams, S.C., David, A.S., 1999. A differential neural response to threatening and non-threatening negative facial expressions in paranoid and non-paranoid schizophrenics. Psychiatry Res. 92, 11–31.
Reetz, K., Dogan, I., Rolfs, A., Binkofski, F., Schulz, J.B., Laird, A.R., Fox, P.T., Eickhoff, S.B., 2012. Investigating function and connectivity of morphometric findings–exemplified on cerebellar atrophy in spinocerebellar ataxia 17 (SCA17). Neuroimage 62, 1354–1366.
Ridgway, G.R., Henley, S.M.D., Rohrer, J.D., Scahill, R.I., Warren, J.D., Fox, N.C., 2008. Ten simple rules for reporting voxel-based morphometry studies. Neuroimage 40, 1429–1435.
Rottschy, C., Langner, R., Dogan, I., Reetz, K., Laird, A.R., Schulz, J.B., Fox, P.T., Eickhoff, S.B., 2012. Modelling neural correlates of working memory: a coordinate-based meta-analysis. Neuroimage 60, 830–846.
Rottschy, C., Caspers, S., Roski, C., Reetz, K., Dogan, I., Schulz, J.B., Zilles, K., Laird, A.R., Fox, P.T., Eickhoff, S.B., 2013. Differentiated parietal connectivity of frontal regions for "what" and "where" memory. Brain Struct. Funct. 218, 1551–1567.
Satterthwaite, T.D., Elliott, M.A., Gerraty, R.T., Ruparel, K., Loughead, J., Calkins, M.E., Eickhoff, S.B., Hakonarson, H., Gur, R.C., Gur, R.E., Wolf, D.H., 2013. An improved framework for confound regression and filtering for control of motion artifact in the preprocessing of resting-state functional connectivity data. Neuroimage 64, 240–256.
Savla, G.N., Vella, L., Armstrong, C.C., Penn, D.L., Twamley, E.W., 2013. Deficits in domains of social cognition in schizophrenia: a meta-analysis of the empirical evidence. Schizophr. Bull. 39, 979–992. http://dx.doi.org/10.1093/schbul/sbs080.
Schilbach, L., Bzdok, D., Timmermans, B., Fox, P.T., Laird, A.R., Vogeley, K., Eickhoff, S.B., 2012. Introspective minds: using ALE meta-analyses to study commonalities in the neural correlates of emotional processing, social & unconstrained cognition. PLoS One 7, e30920.
Seal, M.L., Aleman, A., McGuire, P.K., 2004. Compelling imagery, unanticipated speech and deceptive memory: neurocognitive models of auditory verbal hallucinations in schizophrenia. Cogn. Neuropsychiatry 9, 43–72.
Seeley, W.W., Crawford, R.K., Zhou, J., Miller, B.L., Greicius, M.D., 2009. Neurodegenerative diseases target large-scale human brain networks. Neuron 62, 42–52.
Seiferth, N.Y., Pauly, K., Kellermann, T., Shah, N.J., Ott, G., Herpertz-Dahlmann, B., Kircher, T., Schneider, F., Habel, U., 2009. Neuronal correlates of facial emotion discrimination in early onset schizophrenia. Neuropsychopharmacology 34, 477–487.
Shergill, S.S., Brammer, M.J., Williams, S.C., Murray, R.M., McGuire, P.K., 2000. Mapping auditory hallucinations in schizophrenia using functional magnetic resonance imaging. Arch. Gen. Psychiatry 57, 1033–1038.
Singer, T., Seymour, B., O'Doherty, J., Kaube, H., Dolan, R.J., Frith, C.D., 2004. Empathy for pain involves the affective but not sensory components of pain. Science 303, 1157–1162.
Singer, T., Critchley, H.D., Preuschoff, K., 2009. A common role of insula in feelings, empathy and uncertainty. Trends Cogn. Sci. 13, 334–340.
Skudlarski, P., Jagannathan, K., Calhoun, V.D., Hampson, M., Skudlarska, B.A., Pearlson, G., 2008. Measuring brain connectivity: diffusion tensor imaging validates resting state temporal correlations. Neuroimage 43, 554–561.
Smith, S.M., Nichols, T.E., 2009. Threshold-free cluster enhancement: addressing problems of smoothing, threshold dependence and localisation in cluster inference. Neuroimage 44, 83–98.
Smith, S.M., Vidaurre, D., Beckmann, C.F., Glasser, M.F., Jenkinson, M., Miller, K.L., Nichols, T.E., Robinson, E.C., Salimi-Khorshidi, G., Woolrich, M.W., Barch, D.M., Uğurbil, K., Van Essen, D.C., 2013. Functional connectomics from resting-state fMRI. Trends Cogn. Sci. 17, 666–682.
Sommer, I.E.C., Diederen, K.M.J., Blom, J.-D., Willems, A., Kushan, L., Slotema, K., Boks, M. P.M., Daalman, K., Hoek, H.W., Neggers, S.F.W., Kahn, R.S., 2008. Auditory verbal hallucinations predominantly activate the right inferior frontal area. Brain 131, 3169–3177.
Spreng, R.N., Turner, G.R., 2013. Structural covariance of the default network in healthy and pathological aging. J. Neurosci. 33, 15226–15234.
Sterzer, P., Kleinschmidt, A., 2010. Anterior insula activations in perceptual paradigms: often observed but barely understood. Brain Struct. Funct. 214, 611–622.
Taylor, K.S., Seminowicz, D.A., Davis, K.D., 2009. Two systems of resting state connectivity between the insula and cingulate cortex. Hum. Brain Mapp. 30, 2731–2745.
Thompson, P.M., Cannon, T.D., Narr, K.L., van Erp, T., Poutanen, V.P., Huttunen, M., Lönnqvist, J., Standertskjöld-Nordenstam, C.G., Kaprio, J., Khaledy, M., Dail, R., Zoumalan, C.I., Toga, A.W., 2001. Genetic influences on brain structure. Nat. Neurosci. 4, 1253–1258.
Turkeltaub, P.E., Eickhoff, S.B., Laird, A.R., Fox, M., Wiener, M., Fox, P., 2012. Minimizing within-experiment and within-group effects in Activation Likelihood Estimation meta-analyses. Hum. Brain Mapp. 33, 1–13.
Vigneau, M., Beaucousin, V., Hervé, P.-Y., Jobard, G., Petit, L., Crivello, F., Mellet, E., Zago, L., Mazoyer, B., Tzourio-Mazoyer, N., 2011. What is right-hemisphere contribution to phonological, lexico-semantic, and sentence processing? Insights from a meta-analysis. Neuroimage 54, 577–593.
Wu, C.W., Chen, C.-L., Liu, P.-Y., Chao, Y.-P., Biswal, B.B., Lin, C.-P., 2011. Empirical evaluations of slice-timing, smoothing, and normalization effects in seed-based, resting-state functional magnetic resonance imaging analyses. Brain Connect 1, 401–410.
Wylie, K.P., Tregellas, J.R., 2010. The role of the insula in schizophrenia. Schizophr. Res. 123, 93–104.
Yarkoni, T., Poldrack, R.A., Nichols, T.E., Van Essen, D.C., Wager, T.D., 2011. Large-scale automated synthesis of human functional neuroimaging data. Nat. Methods 8, 665–670.
Zielinski, B.A., Gennatas, E.D., Zhou, J., Seeley, W.W., 2010. Network-level structural covariance in the developing brain. Proc. Natl. Acad. Sci. U. S. A. 107, 18191–18196.
Zu Eulenburg, P., Caspers, S., Roski, C., Eickhoff, S.B., 2012. Meta-analytical definition and functional connectivity of the human vestibular cortex. Neuroimage 60, 162–169.

Please cite this article as: Clos, M., et al., Comparison of structural covariance with functional connectivity approaches exemplified by an investigation of the left anterior i..., NeuroImage (2014), http://dx.doi.org/10.1016/j.neuroimage.2014.05.030